

Gamow-Teller strength in the (p, n) reaction at 136 MeV on ^{20}Ne , ^{24}Mg , and ^{28}Si

B. D. Anderson, N. Tamimi, A. R. Baldwin, M. Elaasar, R. Madey, D. M. Manley,
M. Mostajabodda'vati, J. W. Watson, and W. M. Zhang
Department of Physics, Kent State University, Kent, Ohio 44242

C. C. Foster

Indiana University Cyclotron Facility, Bloomington, Indiana 47408

(Received 23 July 1990)

Gamow-Teller (GT) strength distributions were studied in the (p, n) reaction at 136 MeV on the self-conjugate s - d shell nuclei ^{20}Ne , ^{24}Mg , and ^{28}Si . The measurements were performed in two separate experiments with the beam-swinger neutron time-of-flight facility at the Indiana University Cyclotron Facility. The flight paths were 91 and 131 m, respectively, for the two experiments. The neutrons were detected in large-volume plastic-scintillation detectors. The overall time resolutions were about 825 ps; this provided energy resolutions from 300 to 400 keV. GT strength was identified as $\Delta I=0$ contributions in transitions to discrete final states and also in the background and continuum. The 0° , $\Delta I=0$ cross sections were converted to $B(\text{GT})$ units using a "universal" conversion formula calibrated to (p, n) reactions on other even-even s - d shell nuclei. The resulting $B(\text{GT})$ distributions were compared with full s - d shell-model predictions. The distribution for ^{24}Mg is described well, but the distributions for ^{20}Ne and ^{28}Si are described poorly. The total $B(\text{GT})$ strength observed in discrete states (up to 12 MeV of excitation) for each reaction is $65 \pm 10\%$ of that predicted. If one considers $B(\text{GT})$ strength observed in the continuum above a calculated quasi-free-scattering background, the strength increases to 70–100% of that predicted. If one considers $B(\text{GT})$ strength in an analysis of the full continuum (up to ~ 20 MeV), the entire amount predicted may be observed. These results are consistent with that observed in other light nuclei.

I. INTRODUCTION

The study of Gamow-Teller (GT) strength in nuclei continues to be a topic of high interest. GT transitions involve spin and isospin transfer, and the mapping of such strength in a nucleus provides an important test of structure calculations for that nucleus. The interest in studies of GT strength arises from the fact that such strength is generally "quenched" from that expected by 30–50%. This quenching is seen in beta-decay strengths¹ and also in (p, n) , (p, p') , and (e, e') reaction studies.^{2–5} Various mechanisms have been proposed to explain this quenching, including coupling to Δ -hole excitations, isobar diagrams, and multiparticle-multihole configurational mixing. The amount of quenching and relative contributions to the quenching from these various sources remains uncertain.

Insofar as the (p, n) reaction proceeds predominantly via one-step processes, transitions to 1^+ states from even-even nuclei must proceed via the isovector spin-transfer term of the nucleon-nucleon effective interaction. At low momentum transfer (q), the strengths of these transitions are similar to those of GT beta decays. The usefulness of (p, n) studies of GT strength lies in the fact that the (p, n) reaction, in contrast to beta decay, is not limited by Q -value restrictions and can excite the entire profile of GT strength.

Nuclei in the s - d shell provide excellent cases for the study of GT strength distributions. A number of analog

beta-decay measurements exist that can be used to normalize the strength observed with the (p, n) reaction. This normalization not only calibrates the (p, n) cross sections, but also relates the (p, n) work to the extensive analyses performed on beta decays in the s - d shell nuclei.¹ Also, there exist (p, p') studies of GT strength in s - d shell nuclei that can be compared with the (p, n) measurements.^{6,7} Finally, excellent nuclear structure calculations are available for s - d shell nuclei.⁸ These calculations describe accurately many observables and provide detailed GT strength distributions for comparison with the (p, n) measurements.

In this paper we report the study of GT strength distributions in the (p, n) reaction on ^{20}Ne , ^{24}Mg , and ^{28}Si at 136 MeV. In earlier studies on the s - d shell nuclei ^{18}O , ^{26}Mg , and ^{32}S ,^{9–11} generally good agreement between the experimental results and the shell-model predictions of strength in discrete states was observed with overall normalization factors of about 0.60, a value similar to that required for the beta-decay comparisons in the s - d shell.⁸ The distributions of GT strength were in good agreement with shell-model predictions using the s - d shell-model wave functions of Wildenthal.⁸ The nuclei studied here extend this earlier work to three self-conjugate nuclei in the s - d shell and provide further tests of these shell-model calculations.

Spin-flip excitations in s - d shell self-conjugate nuclei were studied with the (p, p') reaction at 201 MeV.^{6,7} The (p, p') reaction offers both advantages and disadvantages

in the study of GT strength relative to the (p, n) reaction. The (p, p') reaction excites both isovector and isoscalar strength; thus the (p, p') reaction allows one to study quenching in both isovector and isoscalar spin-flip excitations and, possibly, even to look for isospin-mixing effects. The (p, n) reaction excites only isovector strength and provides an unambiguous mapping of such strength. The two reactions complement each other. The (p, p') work of Crawley *et al.*⁷ indicates that the isovector quenching is small ($10\% \pm 10\%$) for these nuclei. This result is surprising and appears to contradict the earlier (p, n) studies and the s - d shell beta-decay analyses. One goal of this work is to compare our (p, n) results with the (p, p') results. The (p, p') studies involve comparison of the observed 1^+ strength with that predicted in distorted-wave impulse approximation (DWIA) calculations using s - d shell-model wave functions.¹² In this work we present a similar analysis for the $^{28}\text{Si}(p, n)^{28}\text{P}$ reaction, in order to compare with the (p, p') analysis.

II. EXPERIMENTAL PROCEDURE

The measurements were performed at the Indiana University Cyclotron Facility with the beam-sweeper system in two separate experimental runs. The first experiment was performed using a ^{28}Si target. The proton beam energy was 135.2 MeV. The second experiment was performed using ^{24}Mg and ^{20}Ne (gas) targets. The beam energy was 135.9 MeV. The experimental arrangement and data-reduction procedures were similar to those described previously.¹³ Neutron kinetic energies were measured by the time-of-flight (TOF) technique. A beam of protons was obtained from the cyclotron in narrow beam bursts typically 350 ps long, separated by 132.7 ns. Neutrons were detected in three detector stations at 0° , 24° , and 45° with respect to the undeflected proton beam. For the purposes of this work, measurements involving only the 0° station were considered. The flight paths were 90.9 and 131.0 m for the first and second experiments, respectively. The neutron detectors were rectangular bars of fast plastic scintillator 10.2 cm thick. For the first experiment, two detectors each 1.02 m long by 25.4 cm high were used in the 0° station. For the second experiment, three detectors each 1.02 m long by 0.51 m high were used in the 0° station. Each scintillator had tapered Plexiglas light pipes attached on the two ends coupled to 12.7-cm-diam phototubes. Timing signals were derived from each end and combined in a mean-timer circuit¹⁴ to provide the timing signal from each detector. Overall time resolutions of about 820 ps were obtained, including contributions from the beam burst width (~ 350 ps) and energy spread (~ 480 ps), energy loss in the target (~ 300 ps), neutron transit times across the 10.2-cm thickness of the detectors (~ 550 ps), and the intrinsic time dispersion of each detector (~ 300 ps). This overall time resolution provided an energy resolution of about 420 keV for the first experiment on ^{28}Si and about 310 keV for the second experiment on ^{20}Ne and ^{24}Mg . The large-volume neutron detectors were described in more detail previously.¹⁵ Protons from the target were rejected by anticoincidence detectors in front of each neutron detector array. Cosmic rays were vetoed by anticoincidence detectors on top as

well as the ones in the front of each array.

The ^{24}Mg and ^{28}Si targets were self-supporting foils 29.2 ± 1.5 and 42.1 ± 0.9 mg/cm² thick, respectively. The ^{20}Ne target was a 4-cm-long gas cell filled to ~ 3 atm (absolute) with 0.5-mil Kapton windows. (Empty-cell "background" runs were performed to subtract the window contributions from the TOF spectra.) Time-of-flight spectra were obtained at approximately 15 angles between 0° and 63° . Spectra from each detector were recorded at many pulse-height thresholds ranging from 25 to 90 MeV equivalent-electron energy (MeVee). Calibration of the pulse-height response of each of the detectors was performed with a ^{232}Th gamma source, which emits a 2.61-MeV gamma ray, and a calibrated fast amplifier. The values of the cross sections extracted for several thresholds (from 40 to 70 MeVee) were found to be the same within statistics.

III. DATA REDUCTION

Excitation-energy spectra were obtained from the measured TOF spectra using the known flight path and a calibration of the time-to-amplitude converter. Known states in the residual nuclei provided absolute reference points. Absolute neutron kinetic energies (and therefore excitation energies) are believed to be accurate to ± 0.1 MeV. The (p, n) excitation-energy spectra at 0.2° for the three targets are shown in Fig. 1.

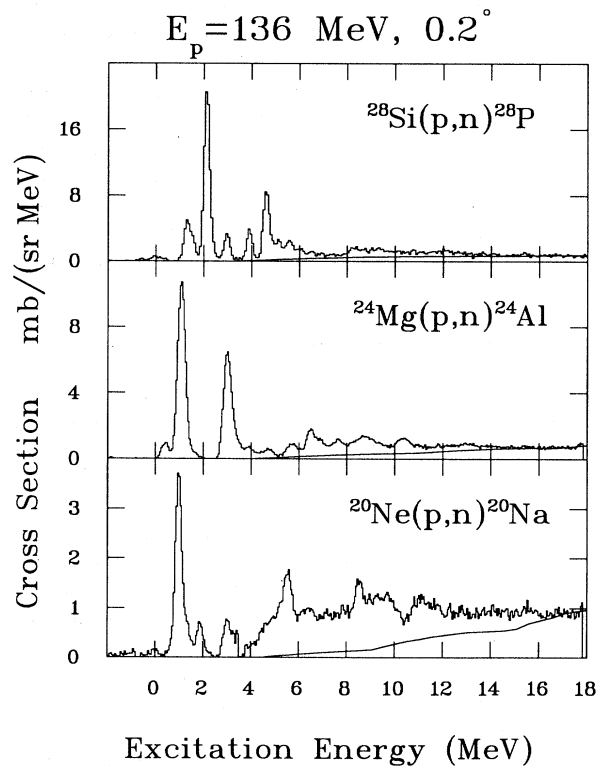


FIG. 1. Excitation-energy spectra for the (p, n) reaction at 136 MeV and 0.2° for targets of ^{20}Ne , ^{24}Mg , and ^{28}Si . The cross sections are in the laboratory system. The normalized quasi-free-scattering background calculations are shown also (see Sec. IV B).

Yields for individual transitions were obtained by fitting the peaks in the TOF spectra. The spectra were fitted with an improved version of the peak-fitting code of Bevington.¹⁶ Examples of peak fitting of similar neutron TOF spectra were presented earlier for the (p,n) reaction on ^{48}Ca and ^{26}Mg .^{13,10} The TOF spectra were subdivided into regions where groups of peaks and a polynomial background could be fitted simultaneously. Cross sections were obtained by combining the yields with the measured geometrical parameters, the beam integration, and the target thickness. The neutron detector efficiencies were obtained from a Monte Carlo computer code,¹⁷ which was tested extensively at these energies.¹⁸ The overall absolute cross sections so obtained were checked by remeasuring the known $^{12}\text{C}(p,n)^{12}\text{N}(\text{g.s.})$ and $^7\text{Li}(p,n)^7\text{Be}$ (0.00+0.43 MeV) cross sections.^{18,19} The experimental procedure and data reduction are similar to those described in more detail in Ref. 13. The uncertainty in the overall scale factor is dominated by the uncertainty in the detector efficiencies and is estimated to be $\pm 12\%$. For a more detailed discussion of the experimental procedure and data reduction, see Ref. 33.

IV. THEORETICAL ANALYSIS AND INTERPRETATION

Gamow-Teller transitions involve no orbital angular momentum transfer ($\Delta l=0$); hence we identify GT strength by the $\Delta l=0$ signature, viz., peaking at 0° . We extracted this GT strength in three steps: (1) First, we fitted each peak with a Gaussian and identified those with $\Delta l=0$ angular distributions as GT transitions. (2) Next, we performed a quasi-free-scattering (QFS) calculation to fit the observed continuum and performed a multipole analysis of the “residual” continuum above this background to obtain the GT strength in this background. (3) We performed a multipole analysis of the entire background and continuum, to obtain an upper limit on the GT strength in the background. Each of these analyses are described more fully below.

A. Gamow-Teller strength in discrete peaks

Gamow-Teller strength in the peaks observed in the 0° spectra (see Fig. 1) was considered first. This strength can be extracted in a relatively unambiguous way.

Cosmic-ray background and “wrap around” of low-energy neutrons from previous beam bursts were subtracted for each TOF spectrum, in a manner similar to that described previously.^{3,11,32} The wrap-around background was approximately one-fifth of the continuum level.^{11,32} We fitted the spectra at each angle simultaneously with Gaussian peaks on a polynomial background. The spectra were fitted in three regions of excitation energy. The minimum number of peaks was used in order to obtain good fits, and care was taken to ensure that the fits changed smoothly from angle to angle. From these fits angular distributions were obtained for all peaks observed in the 0° spectra. The extracted angular distributions for the strongest transition observed in each reaction are shown in Fig. 2, compared with DWIA calculations using s - d shell-model wave functions described below. These

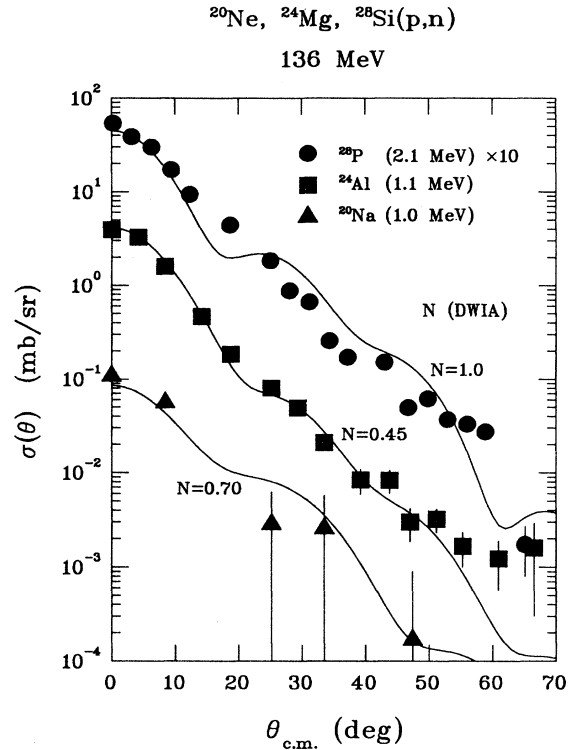


FIG. 2. Angular distributions for the strongest 1^+ transitions in the (p,n) reaction at 136 MeV on ^{20}Ne , ^{24}Mg , and ^{28}Si . The lines represent DWIA calculations using s - d shell-model wave functions (see text). [The $^{28}\text{Si}(p,n)^{28}\text{P}$ cross sections are multiplied by a factor of 10 for clarity in presentation.]

transitions can be followed out to large angles and agree in shape rather well with the calculations.

The amount of $\Delta l=0$ strength in each state was determined from an analysis of the extracted angular distribution for each peak. For the transitions judged to be pure $\Delta l=0$, the strength is taken simply as the cross section at 0° . For mixed transitions, $\Delta l=1$ and/or $\Delta l=2$ shapes were subtracted to obtain the $\Delta l=0$ contributions at 0° . These shapes are discussed below. The resulting $\Delta l=0$ cross sections are presented in Table I. For those peaks that appear to be pure $\Delta l=0$ transitions, the uncertainties are taken from the error matrix of the fitting code. For the mixed transitions, we estimate the uncertainty in the amount of $\Delta l=0$ strength at 0° to be $\pm 30\%$. Because the amount of $\Delta l=0$ strength in mixed transitions is generally a small fraction of the total, the net uncertainties in the total strengths are still small. These are relative uncertainties only. (The absolute uncertainty is dominated by the overall scale uncertainty in the cross sections and is $\pm 12\%$ as discussed above.)

The amount of GT strength associated with the observed $\Delta l=0$ strength is obtained assuming a “universal” relationship between a 0° (p,n) cross section and $B(\text{GT})$ values. This relationship was derived and calibrated earlier for our analysis of the $^{32}\text{S}(p,n)^{32}\text{Cl}$ reaction.¹¹ The relationship takes the form

TABLE I. Gamow-Teller strength in discrete peaks.

E_x (MeV)	$\sigma_{pn}(0^\circ)$ (mb/sr)	$B_{pn}(\text{GT})^a$	E_x (MeV)	$\sigma_{pn}(0^\circ)$ (mb/sr)	$B_{pn}(\text{GT})^a$	E_x (MeV)	$\sigma_{pn}(0^\circ)$ (mb/sr)	$B_{pn}(\text{GT})^a$
$^{20}\text{Ne}(p,n)^{20}\text{Na}$			$^{24}\text{Mg}(p,n)^{24}\text{Al}$			$^{28}\text{Si}(p,n)^{28}\text{P}$		
0.96	1.076(0.007)	0.161	0.44	0.321(0.005)	0.050	1.25	1.407(0.018)	0.180
2.99	0.187(0.004)	0.030	1.07	3.918(0.012)	0.613	1.59	0.776(0.016)	0.100
3.34	0.087(0.004)	0.013	1.58	0.126(0.038) <i>m</i>	0.020	2.10	6.690(0.035)	0.922
4.60	0.042(0.013) <i>m</i>	0.006	2.98	2.312(0.012)	0.362	2.94	0.989(0.017)	0.126
5.50	0.268(0.080) <i>m</i>	0.040	3.33	0.377(0.007)	0.059	3.87	1.144(0.017)	0.137
7.2	0.085(0.023) <i>m</i>	0.013	4.69	0.091(0.027) <i>m</i>	0.015	4.59	2.723(0.024)	0.324
7.5	0.035(0.011) <i>m</i>	0.005	6.46	0.436(0.008)	0.068	5.02	0.888(0.266) <i>m</i>	0.105
7.8	0.127(0.038)	0.019	6.87	0.191(0.008)	0.029	5.55	0.597(0.026)	0.071
8.50	0.100(0.010)	0.015	7.56	0.094(0.028) <i>m</i>	0.015	5.91	0.478(0.014)	0.058
8.93	0.113(0.034) <i>m</i>	0.017	8.48	0.110(0.035) <i>m</i>	0.017	6.50	0.121(0.036) <i>m</i>	0.017
9.28	0.169(0.007)	0.026	8.81	0.126(0.038) <i>m</i>	0.020	8.27	0.278(0.083) <i>m</i>	0.038
9.64	0.155(0.047) <i>m</i>	0.023	10.28	0.188(0.009)	0.029	9.17	0.386(0.116) <i>m</i>	0.053
10.05	0.097(0.009)	0.015	10.95	0.019(0.008)	0.003	10.05	0.298(0.089) <i>m</i>	0.041
10.83	0.138(0.009)	0.021				10.70	0.096(0.029) <i>m</i>	0.014
11.40	0.014(0.004) <i>m</i>	0.002				11.67	0.138(0.041) <i>m</i>	0.019
						12.16	0.219(0.066) <i>m</i>	0.032
						12.59	0.080(0.024) <i>m</i>	0.011
	2.693(0.112)	0.400(0.017)		8.310(0.079)	1.300(0.013)		17.300(0.334)	2.181(0.042)
	$\sum B_{\text{theory}}(\text{GT})=0.510^b$			$=2.325^b$			$=3.757^b$	
	$B_{pn}/B_{\text{theory}}=0.78$			$=0.56$			$=0.58$	

^a $B_{pn}(\text{GT})=\sigma_{pn}(q=0)\times 1/N_D\times 0.064$. See text.

^bFrom full s - d shell-model calculations, $E_x\leq 12$ MeV. See text.

$$B_{pn}(\text{GT})=\frac{\sigma_{pn}(q=0)}{N_D}C_{\text{GT}}, \quad (1)$$

where C_{GT} is a proportionality factor to be obtained by comparison with an analog beta decay. The value of C_{GT} , of course, depends on energy; however, we use it here for only 135 MeV. The distortion factor N_D can be estimated from

$$N_D=\frac{\sigma_{\text{DW}}(0^\circ)}{\sigma_{\text{PW}}(0^\circ)}, \quad (2)$$

where the distorted-wave (DW) and plane-wave (PW) cross sections are calculated with a standard DWIA code.²⁰

In Ref. 11 the factor C_{GT} was evaluated by comparison of the $^{26}\text{Mg}(p,n)^{26}\text{Al}$ (1.06 MeV, 1^+) reaction with the analog beta decay $^{26}\text{Si}(\beta^+)^{26}\text{Al}$ (1.06 MeV, 1^+). The value obtained was

$$C_{\text{GT}}=0.064. \quad (3)$$

The ‘‘universality’’ (i.e., A independence) of this factor was checked by using it to compare $B(\text{GT})$ values obtained from the (p,n) reaction on ^{12}C , ^{14}C , and ^{18}O with analog beta-decay values; the comparisons were all good to within $\pm 7\%$. Evidence was presented also that this factor is constant to $\sim 10\%$ even for heavier nuclei. All of these comparisons are for relatively strong transitions from even-even target nuclei. Certain other cases may

not be described well by Eq. (1). The (p,n) reaction, mediated by the strong nuclear force, is not identical to β decay. Weak transitions are suspect. Two-step processes may be significant in such cases, and these processes may be different in the two reactions. Additionally, there appear to be certain singular transitions, involving odd- A nuclei, which deviate significantly from Eq. (1). These conclusions are similar to, and consistent with, those obtained also by Taddeuci *et al.*, who performed a similar analysis over a wide range of nuclei.² We assume that Eq. (1) applies to the cases of interest here, which involve even-even s - d even nuclei. Following the discussion above, we assume that Eq. (1), using the value of C_{GT} from Eq. (3), is accurate to $\sim \pm 10\%$.

In order to be able to apply Eq. (1), it is necessary to extrapolate each 0° (p,n) cross section to $q=0$ and also to estimate N_D . Both of these tasks were performed using a standard distorted-wave impulse approximation (DWIA) computer code DW81.²⁰ For the extrapolation to $q=0$, calculations were performed for excitation energies in 5-MeV steps, as well as for $Q=0$ (which yields $q=0$). The extrapolation for each state was then interpolated from these calculations. The estimate for N_D was performed with the same code. The optical-model parameters were taken from fits to elastic scattering at 135 MeV by Olmer *et al.* for ^{28}Si .²¹ The plane-wave cross section σ_{PW} was calculated by setting all potential strengths to zero. Because no elastic-scattering analyses are available for ^{20}Ne and ^{24}Mg , N_D was estimated as a smooth interpolation

between N_D for ^{28}Si and N_D calculated for ^{16}O using the optical-model parameters of Kelly.²² From these calculations we estimate $N_D=0.44$, 0.45 , and 0.47 for ^{28}Si , ^{24}Mg , and ^{20}Ne , respectively.

The resulting $B(\text{GT})$ values for these three reactions are listed in Table I. For the $^{20}\text{Ne}(p,n)$ reaction, GT strength is observed in 15 states from 0.96 MeV up to 11.4 MeV in ^{20}Na . The total $B(\text{GT})$ value is 0.40 . For the $^{24}\text{Mg}(p,n)$ reaction, GT strength is observed in 13 states from $E_x=0.44$ MeV up to 11.0 MeV in ^{24}Al . The total $B(\text{GT})$ value is 1.30 . For the $^{28}\text{Si}(p,n)$ reaction, GT strength is observed in 17 states from $E_x=1.25$ MeV up to 12.6 MeV in ^{28}P . The total $B(\text{GT})$ value is 2.18 . [These $B(\text{GT})$ values are all in units where $B(\text{GT})=3.0$ for the beta decay of the free neutron.]

Shown in Fig. 3 are comparisons of these experimental $B(\text{GT})$ values with the shell-model predictions for the GT strength in these three reactions. The shell-model calculations were performed with the computer code OXBASH.²³ The basis assumed for all three cases is the full s - d shell with no restrictions. The two-body matrix elements used were the A -dependent, universal s - d set of Wildenthal.⁸ The wave functions for the initial and final states were used to calculate one-body transition densities (OBTD's), which were then used in the computer code TRANS,¹² which uses one-body GT operators to calculate $B(\text{GT})$ values.

From Fig. 3 one sees that the shell-model calculations reproduce the GT strength distribution well for ^{24}Al , but not well for ^{20}Na or ^{28}P . In ^{24}Al strong excitations are

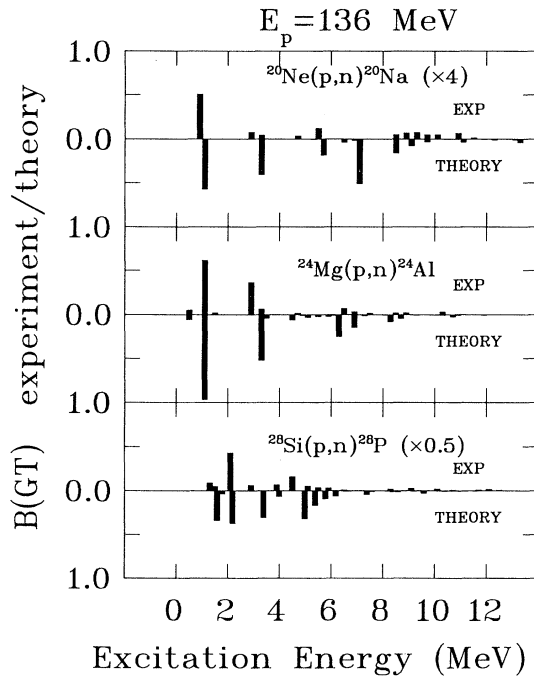


FIG. 3. Comparison of the experimental and shell-model predictions for $B(\text{GT})$ values in the (p,n) reaction on ^{20}Ne , ^{24}Mg , and ^{28}Si . The $^{20}\text{Ne}(p,n)^{20}\text{Na}$ $B(\text{GT})$ values are multiplied by a factor of 4 for presentation.

observed at 1.1 and 3.0 MeV, with a small amount of fragmented strength near 6 MeV; this distribution is reproduced well by the shell-model predictions. In both ^{20}Na and ^{28}P , one state dominates the spectrum experimentally, whereas the shell-model calculations predict three and four strong states, respectively.

In addition to the comparison of the strength distributions, one can consider the integrated, or total, strengths. Experimentally, discrete peaks with GT strength are observed up to about 12 MeV of excitation. In Table I the experimental and predicted strengths up to this excitation energy are compared for these three reactions. Typically, the theoretical sum is over 40 to 50 states. One sees that while the ratio of observed to predicted strength varies, all three are consistent with 0.65 ± 0.13 . This result is consistent also with similar comparisons reported earlier for $^{18}\text{O}/^{18}\text{F}$, $^{26}\text{Mg}/^{26}\text{Al}$, and $^{32}\text{S}/^{32}\text{Cl}$.⁹⁻¹¹ Note that in all these comparisons, the theoretical predictions use the free-nucleon GT operators. These results are consistent also with the analyses of GT beta decays in the s - d shell.¹ As discussed elsewhere,¹¹ if one adopts the “renormalized” effective GT operators of Brown and Wildenthal,¹ the beta decays and (p,n) results on ^{18}O , ^{26}Mg , and ^{32}S can all be described well, with no renormalization.

We see that the summed GT strengths observed in peaks for the three reactions considered here are in good agreement with the earlier (p,n) studies in the s - d shell; however, we see also that the GT *distributions* for two of these three cases are not described well. The poor agreement for the $^{20}\text{Ne}(p,n)^{20}\text{Na}$ reaction might be due to ^{16}O core excitations not considered in the s - d shell-model calculations; however, the GT distribution for the $^{18}\text{O}(p,n)^{18}\text{F}$ reaction was described well, without considering such excitations. The poor agreement for the $^{28}\text{Si}(p,n)^{28}\text{P}$ reaction seems the most problematic. In regard to nucleon filling of orbitals, ^{28}Si is exactly in the middle of the s - d shell, so that one would expect that the important degrees of freedom are in the excited basis. Furthermore, the $^{26}\text{Mg}/^{26}\text{Al}$ and $^{32}\text{S}/^{32}\text{Cl}$ GT distributions are described well. It is possible that “fine tuning” of the interaction used in the shell-model calculations could improve the theoretical descriptions for these two cases;¹² however, such tuning is beyond the scope of this work.

We note that the results obtained here disagree somewhat with those obtained from analysis of 200 -MeV (p,p') studies on these same nuclei reported by Crawley *et al.*⁷ They report ratios of experimentally observed 1^+ strength to theoretically predicted 1^+ strength of $1.00(\pm 0.10)$, $1.13(\pm 0.11)$, and $0.79(\pm 0.10)$, for ^{20}Ne , ^{24}Mg , and ^{28}Si . Their analyses are for peak strengths only and should be comparable with our results. We believe that it is important to try to understand these different results.

The first question is whether the experimental results agree between the (p,n) and (p,p') studies. To this end we compare the observed cross sections for the strongest excited isovector 1^+ states in the (p,n) and (p,p') reactions on ^{20}Ne , ^{24}Mg , ^{28}Si , and ^{32}S . The states considered are the isobaric analogs of each other in each case. If the

TABLE II. Comparison between 136-MeV (p,n) and 201-MeV (p,p') cross sections.

Nucleus	$E_x(p,n)$ (MeV)	$\sigma_{pn}(0^\circ)$ (mb/sr)	$E_x(p,p')$ (MeV)	$\sigma_{pp'}(0^\circ)$ (mb/sr)	$R = \frac{\sigma_{pn}(0^\circ)}{2\sigma_{pp'}(0^\circ)}$
$^{20}\text{Ne}/^{20}\text{Na}$	0.96	1.06 ^a	11.25	0.61 ^b	0.87
$^{24}\text{Mg}/^{24}\text{Al}$	1.08	3.92 ^a	10.72	3.00 ^c	0.65
$^{28}\text{Si}/^{28}\text{P}$	2.1	5.39 ^a	11.45	3.20 ^c	0.84
$^{32}\text{S}/^{32}\text{Cl}$	1.15	1.64 ^d	8.13	1.00 ^c	0.82

^aPresent work.^bReference 6.^cReference 7.^dReference 11.

measurements were performed at the same beam energy, the cross sections should be related simply by the ratio of the isospin geometrical factors. For self-conjugate target nuclei, this ratio should be exactly 2, i.e., $\sigma_{pn} = 2\sigma_{pp'}$. The validity of this relationship has been demonstrated in the comparison of the strongly excited 1^+ GT transition in $A = 12$ and also in comparison of high-spin stretched states in $A = 16$ and 28 .^{24,25} In Table II we present the comparisons of these analog cross sections for the cases of interest here. The (p,p') cross sections are taken from the (extrapolated) 0° values reported by Crawley *et al.*⁷ One sees that, except for $A = 24$, the ratios of $\sigma_{pn}/2\sigma_{pp'}$ are consistently about $0.85(\pm 0.03)$. The fact that this ratio is less than unity is attributed to the energy dependence of the $t_{\sigma\tau}$ term in the isovector central $N-N$ interaction (small) and the difference in the absorptiveness of optical potentials between 135 and 200 MeV. To estimate this ratio, we performed calculations for the strong 1^+ transition in $A = 28$. The calculations were performed with the computer code DW81, with the s - d wave functions for this state. The optical-model parameters were taken from the work of Olmer *et al.*,²¹ who performed elastic-scattering analyses for ^{28}Si from 80 to 180 MeV. These parameters were extrapolated to 201 MeV, and all these extrapolations appear smooth and physical (i.e., no extrapolation was changing rapidly near 180 MeV). Using these calculations, we predict the ratio to be 0.84, in good agreement with that observed for three of the four cases considered. Unfortunately, no reliable elastic-scattering analyses exist over this energy range for the other two nuclei. We conclude that except for $A = 24$, the (p,n) and (p,p') experimental results are in good agreement.

We next consider possible differences in the theoretical analyses of the two experiments. The (p,n) analysis is described above and uses a “universal” conversion factor for converting 0° (p,n) cross sections to $B(\text{GT})$ values. The (p,p') analysis compared the observed 1^+ strength with that predicted by DWIA calculations. The theoretical wave functions employed in these calculations are the same as those described in this work. The DWIA calculations were performed for the first approximately 50 states predicted, which covers the range of excitation energies for which 1^+ states are observed. We considered the case of $A = 28$ only, because good optical-model pa-

rameters (OMP’s) are available. If we perform a similar analysis to that employed in the (p,p') work, we find a ratio of $\sigma_{\text{expt}}/\sigma_{\text{DWIA}} = 0.63$, which is in reasonable agreement with our value of 0.58 for the ratio of $B_{\text{expt}}(\text{GT})/B_{\text{theory}}(\text{GT})$ for this reaction using the universal conversion factor method. Crawley *et al.* obtained 0.79 for this ratio.⁷ With closer analysis we see that the only significant difference in the DWIA calculations appears to be that they used OMP’s from the global parameter set of Schwandt *et al.*,²⁶ while we use the Olmer *et al.* values for ^{28}Si .²¹ We find that the DWIA cross section for the largest 1^+ transition in $^{28}\text{Si}(p,p')$ is 20% smaller if one uses the parameters of Schwandt *et al.* instead of the parameters of Olmer *et al.* This difference removes the discrepancy for the $A = 28$ (p,n) and (p,p') comparisons. We note that the global fit of Schwandt *et al.* is stated to be valid *only* for $A \geq 40$ and $T_p \leq 180$ MeV. In fact, the energy dependence of some of the terms is rising or falling sharply at 180 MeV, so that extrapolation to 200 MeV is questionable. A similar difference probably exists also for the other nuclei considered here and probably largely explains the differences between the (p,n) and (p,p') analyses for all cases, with the exception of ^{24}Mg , which seems to be different by a factor of 2 between (p,n) and (p,p') . Note that ^{24}Mg is also the one case in Table II for which the experimental cross sections do not agree well.

The above discussion points out the need for good optical-model parameters when making absolute comparisons between experiment and theoretical calculations. In the present work, DWIA calculations are needed to extrapolate to $q = 0$ and to estimate N_D . The extrapolation is insensitive to absolute values. The estimate of N_D is more sensitive, but we note that, in the present work, we use optical-model parameters from actual fits to elastic-scattering data on ^{28}Si and ^{16}O , and then interpolate N_D for ^{20}Ne and ^{24}Mg between these values (see earlier discussion).

B. Gamow-Teller strength in the background and continuum

Possible GT strength in the background and continuum was considered in two ways. The first method involves fitting the observed continuum with a plane-wave quasi-free-scattering (QFS) calculation and then perform-

ing a multipole analysis of the background observed above this calculation. The $\Delta l=0$ contribution obtained from that multipole decomposition is identified as possible GT strength. The second method involves performing a multipole decomposition of the entire background and continuum up to the maximum excitation energy observed in this experiment (~ 20 MeV); again, the $\Delta l=0$ contribution is identified as possible GT strength. Both of these methods are described below.

For the first method of considering possible GT strength in the background and continuum, we start by fitting the observed continua with QFS calculations. These calculations were described in detail previously.¹³ The calculations were performed using the plane-wave code of Wu,²⁷ which is based on the formalism of Wolff.²⁸ The calculation uses free nucleon-nucleon scattering cross sections and performs integrations over all possible momenta and angles of the scattered (undetected) proton.

There is a summation over all the single-particle states, each weighted by the number of nucleons in that state. The single-particle wave functions are generated by a subroutine with binding energies obtained from neutron knockout measurements²⁹ and potentials obtained from Elton and Swift.³⁰ The QFS calculations are normalized to fit through the observed continua near $E_x=20$ MeV. Because these are plane-wave calculations, some normalization factor is required. We find that the background and continua near 24° – 30° are described well by these calculations with normalization factors close to the estimated distortion factors (N_D) discussed above. At more forward angles, various giant resonances, including the GT strength and $\Delta l=1$ dipole resonance, are seen clearly above these calculated QFS backgrounds. The required normalization factors decrease from those at 24° – 30° , presumably because of Pauli-blocking effects not adequately modeled in these simple QFS calculations. At

TABLE III. Background Gamow-Teller strength.

	E_x (MeV)	Residual background		Full background	
		$\sigma_{pn}(0^\circ)$ (mb/sr)	B_{pn} (GT)	$\sigma_{pn}(0^\circ)$ (mb/sr)	B_{pn} (GT)
(A) $^{20}\text{Ne}(p,n)^{20}\text{Na}$					
(1)	0.0–2.0	0.000	0.0000	0.000	0.0000
(2)	2.0–4.0	0.000	0.0000	0.000	0.0000
(3)	4.0–6.0	0.085	0.0127	0.169	0.0253
(4)	6.0–8.0	0.141	0.0211	0.282	0.0422
(5)	8.0–10	0.282	0.0422	0.282	0.0422
(6)	10–12	0.352	0.0528	0.422	0.0633
(7)	12–14	0.211	0.0316	0.704	0.1054
(8)	14–16	0.141	0.0211	0.704	0.1054
(9)	16–18	0.004	<u>0.0006</u>	0.020	<u>0.0030</u>
			$\sum B_{pn} = 0.1821$		$\sum B_{pn} = 0.386$
(B) $^{24}\text{Mg}(p,n)^{24}\text{Al}$					
(1)	0.0–2.0	0.000	0.0000	0.000	0.0000
(2)	2.0–4.0	0.000	0.0000	0.000	0.0000
(3)	4.0–6.0	0.157	0.0245	0.220	0.0344
(4)	6.0–8.0	0.471	0.0736	0.314	0.0491
(5)	8.0–10	0.628	0.0982	0.941	0.1473
(6)	10–12	0.471	0.0736	0.941	0.1473
(7)	12–14	0.220	0.0344	0.941	0.1473
(8)	14–16	0.000	0.0211	0.941	0.1473
(9)	16–18	0.000	<u>0.0000</u>	0.003	<u>0.0005</u>
			$\sum B_{pn} = 0.304$		$\sum B_{pn} = 0.673$
(C) $^{28}\text{Si}(p,n)^{28}\text{P}$					
(1)	0.0–2.0	0.000	0.0000	0.000	0.0000
(1)	0.0–2.0	0.050	0.0079	0.050	0.0079
(2)	2.0–4.0	0.044	0.0070	0.088	0.0139
(3)	4.0–6.0	0.877	0.1324	0.175	0.0265
(4)	6.0–8.0	0.135	0.0262	0.175	0.0034
(5)	8.0–10	0.175	0.0324	0.351	0.0647
(6)	10–12	0.175	0.0326	0.438	0.0816
(7)	12–14	0.263	0.0631	0.657	0.1576
(8)	14–16	0.175	0.0418	0.394	0.0940
(9)	16–18	0.000	0.0000	0.393	0.0940
(10)	18–20	0.000	<u>0.0000</u>	0.394	<u>0.0940</u>
			$\sum B_{pn} = 0.343$		$\sum B_{pn} = 0.668$

angles wider than 30° , multistep knockout processes are known to become important, and the single-step background calculated here begins to fall below the observed continua. These wider angles are not important for GT strength studies. The fitted QFS calculations at 0° are shown for each of the three targets in Fig. 1.

These QFS calculations were subtracted from the spectra as well as the peaks which were fitted with the Gaussian peak-fitting code described above. The remaining spectra we refer to as the “residual” background and continua. These residual spectra were binned in 2-MeV intervals to obtain angular distributions. Multipole decompositions were performed for these angular distributions by fitting them with “standard” $\Delta l=0, 1$, and 2 angular distribution shapes. The $\Delta l=0$ shape was obtained from a DWIA calculation for a 0^+ to 1^+ GT transition. The structure assumed is $(d_{3/2}, d_{5/2}^-)$ for the 1^+ final state. The $\Delta l=1$ shape was calculated as a coherent sum of 14 possible 1p-1h configurations which could yield 0^- , 1^- , or 2^- states. This yields an “average” $\Delta l=1$ shape. These shapes were then used to fit the residual background angular distributions in order to determine the $\Delta l=0$ contributions at 0° .

Samples of such fitting were shown previously for ^{48}Ca and ^{54}Fe (p,n) GT analyses.^{3,31} The results of these fits are presented in Table III. As for the peak analyses discussed above, these 0° cross sections are extrapolated to $q=0$ and then converted to $B(\text{GT})$ units with the universal conversion formula. These analyses yield additional $B(\text{GT})$ strength for each reaction corresponding to about 35%, 13%, and 9% of the shell-model predictions for ^{20}Na , ^{24}Al , and ^{28}P , respectively [i.e., $\Sigma B_{\text{theory}}(\text{GT})$ in Table I].

In the second method for considering possible GT strength in the background and continuum, we performed analyses similar to that described above, but for the full continuum and background, i.e., without subtracting a QFS background. Clearly, this method will provide an upper limit to the possible amount of GT strength observed in the region considered (viz., up to $E_x \approx 20$ MeV). The results of the analyses are presented also in Table III. These analyses yield $B(\text{GT})$ strengths for each reaction corresponding to about 75%, 29%, and 18% of the shell-model predicted strength.

We can combine the strengths obtained from these multipole decompositions of the background and continuum with the strengths observed in peaks. For the first method, using a QFS subtraction, we obtain a total $B(\text{GT})$ strength corresponding to 114%, 69%, and 67% of the shell-model predictions for ^{20}Na , ^{24}Al , and ^{28}P , respectively. For the second method, which uses the multipole decomposition of the full background, these fractions increase to 154%, 85%, and 76%.

V. CONCLUSIONS

Gamow-Teller (GT) strength distributions were studied in the (p,n) reaction at 136 MeV on the self-conjugate s - d shell nuclei ^{20}Ne , ^{24}Mg , and ^{28}Si . GT strength was identified as $\Delta l=0$ contributions in transitions to discrete

final states and also in the background and continuum. The 0° , $\Delta l=0$ cross sections were converted to $B(\text{GT})$ units with a “universal” conversion formula calibrated to (p,n) reactions on other even-even nuclei. The resulting $B(\text{GT})$ strengths were compared with s - d shell-model predictions that used the full s - d shell-model space. The comparison between the measured and predicted GT distributions were excellent for $A=24$, but qualitatively poorer for $A=20$ and 28. Similar comparisons performed earlier for the $^{26}\text{Mg}(p,n)^{26}\text{Al}$ and $^{32}\text{S}(p,n)^{32}\text{Cl}$ reactions were in excellent agreement. The poor results for the $A=20$ shell-model calculation may be due to the assumption of a closed ^{16}O core. The poor agreement for the $A=28$ comparison is more puzzling. The $A=28$ systems are in the middle of the s - d shell, and the assumed basis is expected to include all the important degrees of freedom; furthermore, the good agreements observed for similar comparisons with $A=26$ and 32 systems make this result even more surprising.

The total $B(\text{GT})$ strength observed in peaks for each reaction is less than that predicted by the s - d shell-model calculations. The fractions are 78%, 56%, and 58%, respectively, for ^{20}Na , ^{24}Al , and ^{28}P . These results correspond to so-called GT quenching of 22–44%, which agrees with that observed in earlier (p,n) reaction studies. We note that these integral comparisons are generally more reliable than are comparisons for individual transitions; i.e., they are less sensitive to details of the model calculation. The result for the $^{20}\text{Ne}(p,n)^{20}\text{Na}$ reaction appears to be somewhat different than the other two cases and may be a further indication that there is a problem with assuming a closed ^{16}O core for this case.

The results obtained here were compared also with results obtained in (p,p') studies at 201 MeV on the same nuclei. Comparisons of the strongest individual cross sections for each nucleus indicate that the experimental results are in excellent agreement, except possibly for ^{24}Mg , where the (p,n) to (p,p') ratio is about 25% smaller than expected. By comparison with DWIA calculations using the same s - d shell-model wave functions, the (p,p') results are reported to be consistent with no GT quenching, at the $\pm 10\%$ level. We find that this method is sensitive to the optical-model parameters used in the DWIA calculations and that, if we use the parameters of Olmer *et al.* fitted to elastic-scattering results for protons on ^{28}Si , we obtain results about 20% different than the (p,p') analysis for ^{28}Si ; our analysis agrees well with the result obtained using the universal conversion formula method and indicates $> 30\%$ “quenching” for this case.

We considered also possible GT strength in the background and continuum for each reaction. This analysis was performed in two ways. The first method involved subtracting a quasi-free-scattering calculation from the observed continua. The remaining “residual” continua were then divided into 2-MeV intervals and angular distributions formed. Multipole decompositions were performed to obtain the $\Delta l=0$ component at 0° . These $\Delta l=0$ cross sections were then converted to units of $B(\text{GT})$ using the universal conversion formula. These analyses yield additional $B(\text{GT})$ strength for each reaction to yield a total fraction which, when combined with

the peak strengths, yields 114%, 69%, and 67% of the shell-model predictions for ^{20}Na , ^{24}Al , and ^{28}P , respectively. The second method involved performing similar multipole decompositions of the full backgrounds and yields total fractions of 154%, 85%, and 76%, respectively. It is important to realize that these analyses of the background and continua are inherently ambiguous. The analyses are suggestive only; there is no way, at present, to know that this $\Delta I = 0$ strength in the background is definitely GT strength.

The general result obtained here is that $\sim 65\% (\pm 13\%)$ of the shell-model predictions of GT strength is observed in discrete states. This result is consistent with that ob-

served earlier for the *s-d* shell nuclei ^{18}O , ^{26}Mg , and ^{32}S . Consideration of possible GT strength in the background and continua might increase these fractions significantly. Perhaps the most important result of this work is that the large-basis *s-d* shell-model calculations, which can describe the observed GT distributions in ^{18}F , ^{26}Al , and ^{32}Cl so well, do not describe the observed GT distributions in ^{20}Na and ^{28}P well at all. This result is further indication that ^{20}Ne and ^{28}Si are deformed nuclei, not described well by shell-model calculations.

This research was supported in part by the National Science Foundation.

-
- ¹B. A. Brown, W. Chung, and B. H. Wildenthal, *Phys. Rev. Lett.* **40**, 1631 (1978); B. A. Brown and B. H. Wildenthal, *Phys. Rev. C* **28**, 2397 (1983).
- ²T. N. Taddeucci, C. A. Goulding, T. A. Carey, R. C. Byrd, C. D. Goodman, C. Gaarde, J. Larsen, D. Horen, J. Rapaport, and E. Sugarbaker, *Nucl. Phys.* **A469**, 125 (1987).
- ³B. D. Anderson, T. Chittrakarn, A. R. Baldwin, C. Lebo, R. Madey, P. C. Tandy, J. W. Watson, B. A. Brown, and C. C. Foster, *Phys. Rev. C* **31**, 1161 (1985).
- ⁴N. Marty, in *Weak and Electromagnetic Interactions in Nuclei*, edited by H. V. Klapdor (Springer-Verlag, Berlin, 1986), p. 268.
- ⁵A. Richter, *Nucl. Phys.* **A374**, 177c (1983).
- ⁶A. Willis, M. Morlet, N. Marty, C. Djalali, G. M. Crawley, A. Galonsky, V. Rotberg, and B. A. Brown, *Nucl. Phys.* **A464**, 315 (1987).
- ⁷G. M. Crawley, C. Djalali, N. Marty, M. Morlet, A. Willis, N. Anantaraman, B. A. Brown, and A. Galonsky, *Phys. Rev. C* **39**, 311 (1989).
- ⁸B. H. Wildenthal, *Prog. Nucl. Phys.* **11**, 5 (1984).
- ⁹B. D. Anderson, A. Fazely, R. J. McCarthy, P. C. Tandy, J. W. Watson, R. Madey, W. Bertozzi, T. N. Buti, J. M. Finn, J. Kelly, M. A. Kovash, B. Pugh, B. H. Wildenthal, and C. C. Foster, *Phys. Rev.* **27**, 1387 (1983).
- ¹⁰R. Madey, B. S. Flanders, B. D. Anderson, A. R. Baldwin, C. Lebo, J. W. Watson, S. M. Austin, A. Galonsky, B. H. Wildenthal, and C. C. Foster, *Phys. Rev. C* **35**, 2011 (1987).
- ¹¹B. D. Anderson, T. Chittrakarn, A. R. Baldwin, C. Lebo, R. Madey, P. C. Tandy, J. W. Watson, C. C. Foster, B. A. Brown, and B. H. Wildenthal, *Phys. Rev. C* **36**, 2195 (1987).
- ¹²B. A. Brown (private communication).
- ¹³B. D. Anderson, T. Chittrakarn, A. R. Baldwin, C. Lebo, R. Madey, R. J. McCarthy, J. W. Watson, B. A. Brown, and C. C. Foster, *Phys. Rev. C* **31**, 1147 (1985).
- ¹⁴A. R. Baldwin and R. Madey, *Nucl. Instrum. Methods* **214**, 401 (1983).
- ¹⁵R. Madey *et al.*, *Nucl. Instrum. Methods* **214**, 401 (1983).
- ¹⁶P. R. Bevington, *Data Reduction and Error Analysis for the Physical Sciences* (McGraw-Hill, New York, 1969), p. 237.
- ¹⁷R. Cecil, B. D. Anderson, and R. Madey, *Nucl. Instrum. Methods* **161**, 439 (1979).
- ¹⁸J. W. Watson, B. D. Anderson, A. R. Baldwin, C. Lebo, B. Flanders, W. Pairsuwan, R. Madey, and C. C. Foster, *Nucl. Instrum. Methods* **215**, 413 (1983).
- ¹⁹J. D'Auria, M. Dombisky, L. Moritz, T. Ruth, G. Sheffer, T. E. Ward, C. C. Foster, J. W. Watson, B. D. Anderson, and J. Rapaport, *Phys. Rev. C* **30**, 1999 (1984).
- ²⁰R. Schaeffer and J. Raynal, Program DWBA70 (unpublished); J. R. Comfort, extended version DW81 (unpublished).
- ²¹C. Olmer, A. D. Bacher, G. T. Emery, W. P. Jones, D. W. Miller, H. Nann, P. Schwandt, S. Yen, T. E. Drake, and R. J. Sobie, *Phys. Rev. C* **29**, 361 (1984).
- ²²J. Kelly, Ph.D. dissertation, Massachusetts Institute of Technology, 1981 (unpublished).
- ²³B. A. Brown, A. Etchegoyen, W. D. M. Rai, and N. S. Godwin, program OXBASH (unpublished).
- ²⁴A. Fazely, B. D. Anderson, M. Ahmad, A. R. Baldwin, A. M. Kalenda, R. J. McCarthy, J. W. Watson, R. Madey, W. Bertozzi, T. N. Buti, J. M. Finn, M. A. Kovash, B. Pugh, and C. C. Foster, *Phys. Rev. C* **25**, 1982.
- ²⁵A. Fazely, R. Madey, B. D. Anderson, A. R. Baldwin, C. Lebo, P. C. Tandy, J. W. Watson, W. Bertozzi, T. Buti, M. Finn, C. Hyde-Wright, J. Kelly, M. A. Kovash, B. Murdock, B. Pugh, and C. C. Foster, *Nucl. Phys.* **A443**, 29 (1985).
- ²⁶P. Schwandt, H. O. Meyer, W. W. Jacobs, A. D. Bacher, S. E. Vigdor, M. D. Kaitchuck, and T. R. Donoghue, *Phys. Rev. C* **26**, 55 (1982).
- ²⁷J. R. Wu, *Phys. Lett.* **91B**, 169 (1980).
- ²⁸P. A. Wolff, *Phys. Rev.* **87**, 434 (1952).
- ²⁹J. W. Watson, P. J. Pella, M. Ahmad, B. S. Flanders, N. S. Chant, P. G. Roos, D. W. Devins, and D. L. Friesel, *J. Phys. (Paris) Colloq.* **45**, C4-91 (1984).
- ³⁰L. R. B. Elton and A. Swift, *Nucl. Phys.* **A94**, 52 (1967).
- ³¹B. D. Anderson, C. Lebo, A. R. Baldwin, T. Chittrakarn, R. Madey, J. W. Watson, and C. C. Foster, *Phys. Rev. C* **41**, 1474 (1990).
- ³²T. Chittrakarn, B. D. Anderson, A. R. Baldwin, C. Lebo, R. Madey, J. W. Watson, and C. C. Foster, *Phys. Rev. C* **34**, 80 (1986).
- ³³N. Tamimi, Ph.D. Dissertation, Kent State University, 1989 (unpublished).